

No Planet around the K Giant Star 42 Draconis [★]

A. P. Hatzes¹, V. Perdelwitz², M. Karjalainen³, J. Köhler¹, M. Hartmann¹, and M. Endl⁴

¹ Thüringer Landessternwarte Tautenburg, Sternwarte 5, D-07778 Tautenburg, Germany
e-mail: artie@tls-tautenburg.de

² Department of Earth & Planetary Sciences, Weizmann Institute of Science, Rehovot 76100, Israel
e-mail: volker.perdelwitz@weizmann.ac.il

³ Astronomical Institute, Czech Academy of Sciences, 251 65, Ondrejov, Czech Republic e-mail: marie.karjalainen@asu.cas.cz

⁴ McDonald Observatory, The University of Texas at Austin, Austin, TX 78712, USA e-mail: mike@astro.as.utexas.edu

Received; accepted

ABSTRACT

Context. Published radial velocity measurements of the K giant star 42 Dra taken over a three year time span reveal variations consistent with a $3.9 M_{Jup}$ mass companion in a 479-d orbit.

Aims. This exoplanet can be confirmed if these variations are long-lived and coherent. Continued monitoring may also reveal additional companions.

Methods. We have acquired additional radial velocity measurements of 42 Dra so that the data now span fifteen years. Standard periodogram analyses were used to investigate the stability of the planet radial velocity signal. We also investigated variations in the spectral line shapes using the bisector velocity span as well as infrared photometry from the COBE mission.

Results. The recent radial velocity measurements do not follow the published planet orbit. An orbital solution using the 2004 - 2011 data yields a period and eccentricity consistent with the published values, but the radial velocity amplitude has decreased by a factor of four from the earlier measurements. Including some additional radial velocity measurements taken between 2014 and 2018 reveal a second period at 530 d. The beating of this period with the one at 479-d may account for the observed amplitude variations. The planet hypothesis is conclusively ruled out by COBE/DIRBE 1.25μ photometry that shows variations with the planet orbital period as well as a 170 d period.

Conclusions. The radial velocity of 42 Dra shows significant amplitude variations which along with the COBE/DIRBE photometry firmly established that there is no giant planet around this star. The presence of multi-periodic variations suggests that these we are seeing stellar oscillations in this star, most likely oscillatory convection modes. These oscillations may account for some of the long period radial velocity variations attributed to planets around K giant stars which may skew the statistics of planet occurrence around intermediate mass stars. Long-term monitoring with excellent sampling is required to exclude amplitude variations in the long-periods found in radial velocity of K giant stars.

Key words. star: individual: 42 Dra, - techniques: radial velocities - stars: late-type - planetary systems

1. Introduction

Radial velocity (RV) surveys of K-giant stars have shown to be effective means of probing planet formation around intermediate-mass (IM) stars with masses 1.3 to $2 M_{\odot}$. These measurements for IM main sequence stars are not conducive for RV planet search surveys, since A to early F stars have high effective temperatures which results in relatively few spectral lines. These stars also tend to have high rates of rotation. Few and broad spectral lines results in an RV precision of several tens to hundreds $m s^{-1}$ making the detection of sub-stellar companions difficult. On the other hand, intermediate-mass stars that have evolved up the giant branch have cooler effective temperatures, thus more spectral lines, and much slower rotation

rates. They are thus highly amenable to Doppler surveys for planet searches. There have been several studies been for planetary companions to K giant stars with the Doppler method (e.g. Frink et al. 2002; Setiawan et al. 2003; Döllinger et al. 2007; Johnson et al. 2007; Sato et al. 2008; Niedzielski et al. 2009; Wittenmyer et al. 2011; Jones et al. 2011, Lee et al. 2012). These surveys have discovered over 100 giant planets around IM evolved stars.

However, K giants have their own disadvantages for Doppler surveys. First, these stars have p -mode oscillations which introduce intrinsic variations in the form of RV jitter. The amplitudes are proportional to the luminosity of the star (Kjeldsen & Bedding 1995), so this RV jitter becomes larger as one moves up the giant branch. For stars near the bottom of the giant branch this is as low as a few $m s^{-1}$ and can be as high as tens of $m s^{-1}$ for a more evolved star.

[★] Based in part on observations obtained at the 2-m-Alfred Jensch Telescope at the Thüringer Landessternwarte Tautenburg

Second, they can exhibit rotational modulation due to stellar structure most likely associated with magnetic activity. The expected rotational periods are several hundreds of days, comparable to the orbital periods found for many stellar companions to K giant stars. The first hint for rotational modulation induced RV variations was in α Boo. Hatzes & Cochran (1993) found RV variations with a period of 231 d, nearly identical to the 233 d rotational period inferred from He I 10830 Å variations by Lambert (1987). Finally, these stars may have new and unknown types of oscillations.

Unfortunately, we know very little about activity and stellar structure on slowly rotating single giant stars, or even the presence of long-period oscillations. To exclude the possibility of rotational modulation as a source of the RV variability, most investigators look for variations in standard activity indicators. These include photometry, often utilizing the archive photometry from the astrometric space mission HIPPARCOS, Ca II H & K, the Ca II infrared triplet, or H α (e.g. Hatzes et al. 2015). If variations are found in any of these indicators with the same period as the RV variations, then serious doubt is cast on the planet hypothesis.

Stellar line bisectors have also become a common tool for proving the planet hypothesis. If any surface inhomogeneities (spots, abundance, convective velocities, etc.) are present then these should be accompanied by variable distortions in the spectral line shapes. Indeed, it is these line distortions that mimic an RV variation by causing a shift in the centroid of the spectral line as the star rotates. Line bisector measurements were used to show that the RV variations of HD 166435 were due spots rather than a short-period giant planet (Queloz et al. 2001) as well as to confirm the planet hypothesis for 51 Peg b (Hatzes et al. 1998).

Spectral line bisector variations generally require spectra taken at very high resolving power ($R = \lambda/\delta\lambda \geq 100\,000$). With data taken at lower spectral resolutions a lack of bisector variations is a necessary condition to confirm a planet, but it is by no means a sufficient one. A case in point is the purported planet around TW Hya. RV measurements showed evidence for the presence of a short-period Jupiter-mass planet around this T Tauri star (Setiawan et al. 2008). These measurements were taken at reasonably high resolution (resolving power, $R = \lambda/\delta\lambda = 45\,000$). An observed lack of a correlation between the RV and the spectral line bisector variations presumably “confirmed” the planet. However, subsequent RV measurements taken in the infrared showed that these had one-third the amplitude of the optical measurements (Huélamo et al. 2008). The periodic RV signal was clearly due to spots.

So, the generally accepted procedure for confirming the planetary nature of periodic RV signal is to look at as many ancillary data as possible. If one does not see the RV period in any of these, then the planet hypothesis is “confirmed”. However, for giant stars this lack of variability may lead to wrong conclusions.

In an extensive study of Aldebaran, Hatzes et al. (2015) analyzed 30 years of RV data for this star. These seemed to show a long-lived periodic signal at 629-d that was interpreted as a due to a planetary companion. There were no variations at the 629-d RV period in the equivalent widths of the activity

indicators H α or Ca II λ 8662, HIPPARCOS photometry or in the spectral line shapes. An additional, intermittent signal at 520-d was seen in the RV residuals, H α and Ca II and at one-third this period in the spectral line bisectors. The planet hypothesis was the logical conclusion. However, Reichert et al. (2019) argued against the planet hypothesis based on additional RV measurements. These showed that the \sim 620-d period had phase shifts and there were times when it was not present at all.

The K giant star γ Dra also showed evidence for a “fake” planet. Seven years of RV measurements showed coherent, long-lived periodic variations at 702 d consistent with an 11 M_{Jup} (Hatzes et al. 2018). The lack of variability at this period in the Ca II S-index, spectral line shapes, and HIPPARCOS photometry seemed to support the planet hypothesis. In fact, the authors were preparing a paper as a planet discovery around γ Dra when more RV measurements spanning an additional two years became available. These showed that the 702-d period disappeared during 2011-2017, only to return in 2014 but with a phase shift. This behavior was reminiscent to that seen in Aldebaran and thus refuted the planet hypothesis.

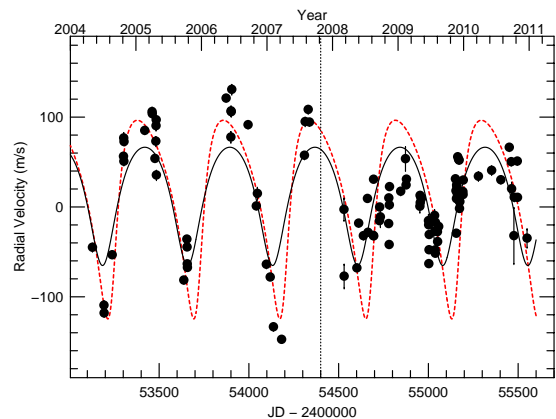


Fig. 1. The RV measurements for 42 Dra. The vertical dashed line marks the boundary between the old and new RV measurements. The dashed curve is the orbital solution from D09 and the solid curve a new solution based on all the 2004 – 2011 data.

At the Thüringer Landessternwarte Tautenburg (TLS) we have been monitoring a sample of K giant stars with the Doppler method to search for exoplanet companions. This program has resulted in discoveries of the planetary companions around 4 UMa (Döllinger et al. 2007), 42 Dra and HD 139357 (Döllinger et al. 2009a; hereafter D09), 11 UMi, and HD 32518 (Döllinger et al. 2009b). RV measurements of the giant star 42 Dra varied with a period 479.1 d and a K -amplitude of $K = 110.5 \text{ m s}^{-1}$. This was consistent with the presence of a sub-stellar companion with a minimum mass of $3.9 M_{Jup}$. HIPPARCOS photometry showed no variations with the RV period. Furthermore, the RV signal seemed to be relatively long-lived and coherent having the same amplitude for almost three full orbital periods, or about 3.3 years. No bisector measurements were performed on the star, but measurements of the

equivalent width of the $H\alpha$ line showed no correlation with the RV data. The RV variations showed all the earmarks of stemming from a planetary companion.

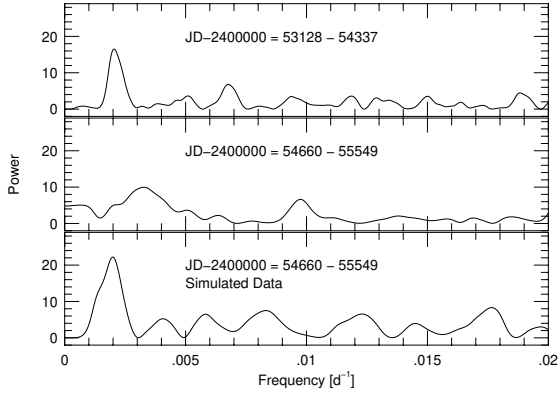


Fig. 2. (Top) The Lomb-Scargle periodogram of the RV measurements up to JD = 2454337. (Middle) The periodogram of the RV measurements taken after JD \approx 2454660. (Bottom) The periodogram of a simulated orbit over the same time range as the middle panel. The 479-d should have been present in the periodogram of the latter RV measurements.

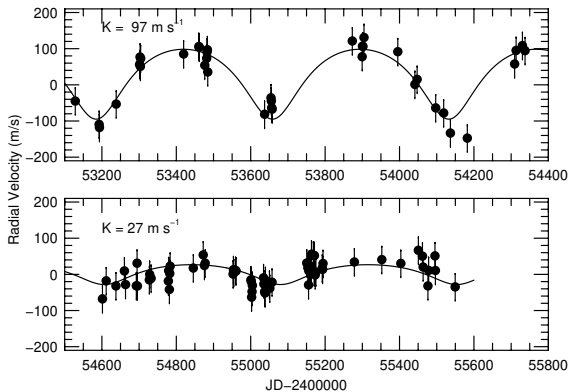


Fig. 3. (Top) The orbital solution of the data up to JD \approx 2454400. The K -amplitude is 96 m s^{-1} . (Bottom) An orbital solution to the RV data taken from JD \approx 2454400 – 2455600. All orbital parameters except the RV amplitude were kept fixed for both data subsets. The K -amplitude for the latter data is 27 m s^{-1} .

We continued to monitor 42 Dra with RV measurements for an additional nine years, three of these with good cadence. This was not only to confirm the planet hypothesis for the 479-d variations (given the experience with Aldebaran and γ Dra), but also to look for additional companions. An examination of the infrared photometry from the COBE mission was also made. All these show that the RV variations seen in 42 Dra do not

arise from the orbital reflex motion of the host star due to a sub-stellar companion.

2. Stellar parameters

Since stellar parameters for evolved stars are often not included in catalogs like Gaia (Gaia collaboration et al. 2021) or the TESS Input Catalog (Paegert et al. 2021), we derived these values using the open-source package *Stellar Parameters of Giants and more* (Stock et al. 2018). SPOG+ uses Bayesian inference along with observational data to derive fundamental stellar properties, which are listed in Table 1 with the input parameters and their sources. All parameters are very well-constrained, and we found that they are in good agreement with those stated in other papers (e.g. Yu et al. 2023; Khalatyan et al. 2024).

The stellar radius from SPOG+ also agrees well with the radius measured from via interferometry. Baines et al. (2018) measured an angular diameter of $2.048 \pm 0.009 \text{ mas}$ for 42 Dra. Using the Gaia parallax this results in a stellar radius of $R = 19.78 \pm 0.17 R_{\odot}$.

3. Data Acquisition

In the time span 2008 – 2011 observations were made with very good cadence using the Tautenburg Coude Echelle Spectrograph (TCES) of the 2-m Alfred Jensch Telescope. The spectral data covered a wavelength region of 4700 \AA to 7400 \AA at a spectral resolving power of $R = 67\,000$. An iodine absorption cell placed in the optical path was used to provide the wavelength reference for the precise stellar RVs (see Hatzes et al. 2005).

Between 2014 to 2018 additional measurements were made but at much reduced cadence. These were also taken with a different instrumental setup, namely a new echelle grating and a new CCD detector. These data will have a different zero point offset compared to the 2008 – 2011 measurements.

Table 2 lists the RV measurements from 2004 – 2011. These include values derived from previous published data. Since the RV analysis was done on the full data set values will differ from the values published in D09. Table 3 is for the RV measurements from 2014 – 2018. RVs were produced with the pipeline *viper* (Zechmeister et al. 2021).

Our approach is to first examine the data taken in 2008 – 2011 when the “planet” signal was present to see if these give early hints that it is not a planet. RV measurements in the final years are added to the analysis to shed light on the true nature of the RV variations.

4. Results

Figure 1 shows the RV measurements from 2004 – 2011 as well as the orbital solution of D09 whose parameters are $P = 479.1 \pm 6.2 \text{ d}$, $e = 0.38 \pm 0.06$, $\omega = 218.7 \pm 10.6 \text{ degrees}$, and $K = 110.5 \pm 10.6 \text{ m s}^{-1}$. Clearly, the measurements taken from JD = 2454600 to 2455600 do not fit the orbit.

We performed an orbital solution using the 2004 - 2011 data set. The parameters are listed in Table 4. The period and

eccentricity agree with the orbital solution of D09, but the full data yield a slightly shorter period of 474 d. (In the discussion that follows we will refer to the planet period by its original value of 479 d). Overall, one could still conclude that the signal of the planetary companion was present for at least seven years. However, there is a discrepancy in that the current K -amplitude (65 m s^{-1}) is nearly a factor of two smaller than the earlier K -amplitude of 110 m s^{-1} .

4.1. Amplitude Variations

We investigated whether the high cadence data from 2004 – 2011 alone were sufficient to provide strong evidence against the planet hypothesis. The top panel of Figure 2 shows the Lomb-Scargle (L-S) periodogram (Scargle 1982) of the data up to JD = 2454337. One sees the significant signal at a frequency of $\nu = 0.0021 \text{ d}^{-1}$, near the orbital frequency that was first reported in D09. On the other hand, the periodogram for the RV data from JD = 2454660 – 245549 shows no significant peak at the planet orbital period (central panel). The strongest peak actually is at $\nu = 0.00327 \text{ d}^{-1}$ ($P = 305 \text{ d}$) and is modestly significant (false alarm probability $\approx 0.3 \%$).

We checked whether the original 479 d period could have been detected in the RV data JD = 2454660 – 245549 if it were indeed present. We sampled the original orbital solution shown in Figure 1 in the same manner as the real data and added noise at a level of 55 m s^{-1} . This value is much higher than our typical measurement error, but it is the level of the scatter about the orbital solution. It is also consistent with the level of RV jitter expected from stellar oscillations in this star (see below).

The lower panel of Figure 2 shows the periodogram of the synthetic data, but only using those time stamps from the middle panel. Clearly, we should have easily detected the orbital motion even when using only the new RV measurements.

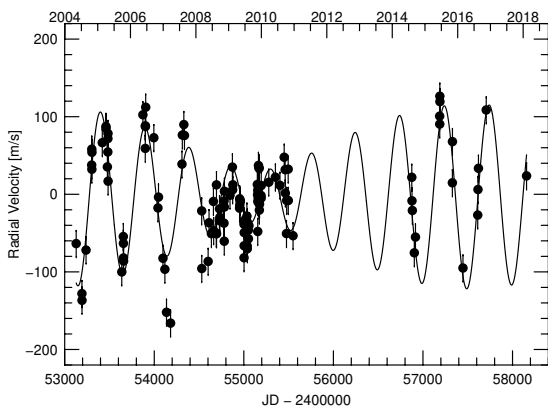


Fig. 4. The complete RV measurements of 42 Dra from 2004 – 2018 (points). The curve represents a two-component fit with two periods, $P_1 = 487.3 \text{ d}$ and $P_2 = 530 \text{ d}$.

The RV data show a clear variation in the amplitude of the 479-d signal. We took our revised orbital solution and used the

parameters to fit the RV data up to JD = 2454530. All parameters were kept fixed and only the K -amplitude was allowed to vary. This resulted in $K = 96.6 \pm 6.3 \text{ m s}^{-1}$ (upper panel of Fig. 3). We then fit the RV data taken after JD = 245660 again allowing only the RV amplitude to vary. (We removed two data points in the fit in order to provide a larger time gap between the two subset data.) This resulted in $K = 27.4 \pm 6.1 \text{ m s}^{-1}$ (lower panel of Fig. 3). If the 479-d period were present, its RV amplitude has been reduced by about a factor of four from the earlier measurements. This is inconsistent with the orbital reflex motion of the host star due to a companion.

4.2. Frequency Analysis of the Full Data Set

We then performed a frequency analysis of the full RV data set covering JD = 2453128 – 2458156 (2004 – 2018) that is shown in Figure 4. This was done using a pre-whitening procedure. Periodic signals were sequentially found and subtracted and a search for additional signals was made on the residuals. The process was stopped when the final peak had a false alarm probability, $FAP < 0.01$. The FAP was estimated from the height of the peak compared to the surrounding noise level (i.e. the signal-to-noise ratio, SNR). This SNR can be converted into a FAP (Kuschnig et al. 1997; Hatzes 2019). Three significant frequencies were found, shown in Table 5. The curve in Figure 4 shows a fit to the RV data using the first two periods (487-d and 530-d) which better shows the beating between these two dominant periods.

4.3. An Examination of the Indicators for Planet Confirmation

As discussed in the introduction, it is wise to look for variations with the RV period in other quantities. If these show variations with the same period as the RV, then the planet hypothesis can be rejected. D09 examined the equivalent width of $H\alpha$ in 42 Dra and found no variations with the RV period, but the authors did not investigate any line shape variations. Here we take a closer look at the spectral line shapes as well as HIPPARCOS photometry.

4.3.1. Spectral Line Shape Variations

To investigate changes in the spectral line shapes we calculated the cross-correlation function (CCF) using the spectral region 4790–4900 Å and the first observation as a template. This region is largely free of the iodine absorption lines that we use for our wavelength calibration. We then calculated the bisector of the CCF – the locus of the midpoints calculated from both sides of the CCF having the same flux value. A linear least-squares fit was then made to the CCF bisectors. We finally converted this slope between the CCF height values of 0.3 to 0.85 to an equivalent velocity which we will call the bisector velocity span (BVS).

The top panel of Fig. 5 shows the L-S periodogram of the BVS measurements for 2004 to 2011 when the planet signal was present. There is a modest peak at a frequency of $\nu =$

$0.001497 \pm 0.000060 \text{ d}^{-1}$ ($P = 671 \pm 28 \text{ d}$) with an amplitude of $\approx 60 \text{ m s}^{-1}$. This frequency is significantly different from the orbital frequency of the purported planet. A bootstrap analysis (see below) indicates a relatively low FAP of $\approx 5 \times 10^{-4}$. The crucial point is that the BVS frequency does not coincide with the orbital frequency.

4.3.2. Hipparcos photometry revisited

D09 showed that there were no significant variations in the HIPPARCOS photometry with the same period as the RV variations. We took another look at the HIPPARCOS photometry to see if there were any low frequency signals in the data that could possibly coincide with the BVS variations. The lower panel of Fig. 5 shows the low frequency end of L-S periodogram of the HIPPARCOS photometry. There is indeed a peak at $\nu = 0.00145 \pm 0.00018 \text{ d}^{-1}$ ($P = 690 \pm 90 \text{ d}$) that is consistent with the one seen in the BVS, but the signal is not very significant (FAP ~ 0.05). The HIPPARCOS photometry does not refute the planet hypothesis.

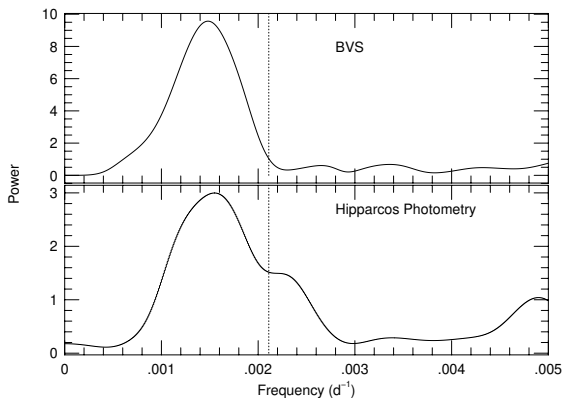


Fig. 5. (Top) The Lomb-Scargle periodogram of the bisector velocity span (BVS) during the time when the planet signal was present. (Bottom) The Lomb-Scargle periodogram of the HIPPARCOS photometry. We should note that the photometry was not contemporaneous with the BVS measurements. The dashed vertical line is the orbital frequency of the purported planet.

4.4. DIRBE Photometry: Final Refutation of the Planet Hypothesis

Price et al. (2010) extracted weekly average near infrared fluxes for 2652 stars in the all-sky maps of the Diffuse Infrared Background Experiment on the Cosmic Background Explorer (COBE/DIRBE); hereafter “DIRBE photometry”). We used the time series of $1.25 \mu\text{m}$ fluxes for 42 Dra to search for periodic signals. Figure 6 shows the L-S periodogram of the DIRBE photometry. The strongest peak coincides with the orbital frequency of the planet shown by the vertical dashed line. There is

a second strong peak at $\nu = 0.00589 \text{ d}^{-1}$ ($P = 169.8 \text{ d}$). Figure 7 shows the DIRBE photometry phased to the 479-d period.

We assessed the false alarm probability (FAP) using the bootstrap method (Murdoch et al. 1993). In this method the RV data are randomly shuffled a large number (10^5) of times keeping the time stamps fixed. The fraction of random power larger than the data power yields the FAP. Since we are interested in the FAP at a known frequency in the data we employed a “windowing” bootstrap (Hatzes 2019). The FAP is determined via bootstrap over a modest sized window centered on the frequency of interest. The window is then successively narrowed and a new FAP calculated. The final FAP is the extrapolated value at zero width for the window at the frequency of interest. This resulted in a FAP $\approx 2 \times 10^{-3}$ that random noise could produce the observed power *exactly* at the planet orbital frequency.

We also assessed the FAP of the second peak using the bootstrap, but over a larger frequency range $\nu = 0 - 0.02 \text{ d}^{-1}$ since the 169.8-d period is not a known signal. After removing the contribution of the 479-d signal we found a FAP ≈ 0.01 that a peak would have higher power anywhere in the frequency range of interest.

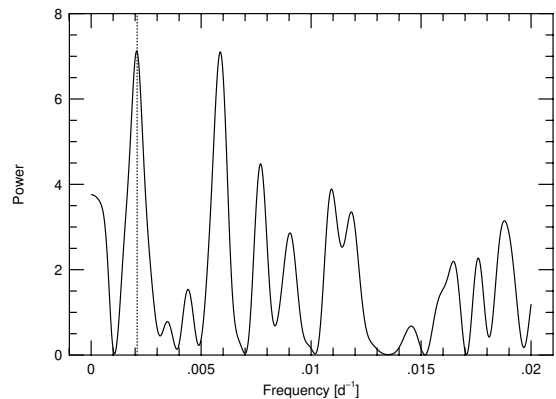


Fig. 6. Lomb-Scargle periodogram of the DIRBE $1.25 \mu\text{m}$ photometry. The dashed vertical line is the orbital frequency of the purported planet.

4.5. Short-term RV variations

As part of our study of 42 Dra we investigated the short term RV variability by observing the star with high cadence over several nights. Figure 8 shows the best time series from these observations (RV values are listed in Table 6).

It is beyond the scope of this paper for a detailed study of the short term variations - our observations are too sparse. Nevertheless, we performed a frequency analysis to assess the rough time scales and amplitudes involved. This resulted in two dominant signals, one with frequency $\nu_1 = 0.768 \text{ d}^{-1}$ ($P_1 = 1.3 \text{ d}$) and RV amplitude $K_1 = 79.3 \text{ m s}^{-1}$ and $\nu_2 = 1.21 \text{ d}^{-1}$ ($P = 0.82 \text{ d}$) and RV amplitude $K_2 = 49.2 \text{ m s}^{-1}$. The curve in the figure shows the two-component fit.

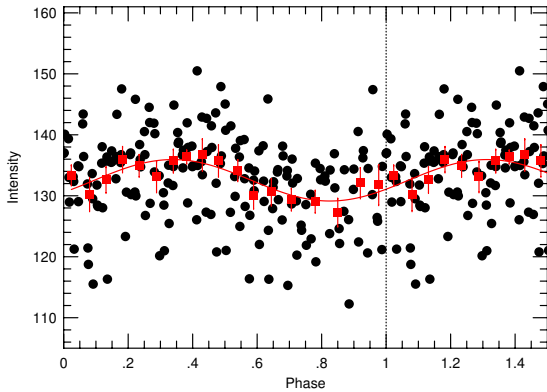


Fig. 7. The DIRBE photometry phased to the 479-d “orbital” period. The red squares are phase-binned values. The curve represents a sine fit to the data. Data measurements are repeated to the right of the vertical dashed line.

Clearly, these are p-mode oscillations. Kjeldsen & Bedding (1995) gave simple scaling relations for the frequency of maximum power, v_{max} , and amplitudes for these stellar oscillations. Using the stellar parameters of 42 Dra, these scaling relationships give $v_{max} \approx 0.88 d^{-1}$ ($P = 1.14$ d), close to our value for ν_1 . These relationships also give a predicted velocity amplitude of ≈ 30 m s $^{-1}$.

Kjeldsen & Bedding (2011) gave revised scaling relations for the oscillation amplitude taking into account the stellar temperature and with a stronger dependence on the stellar mass. These require a knowledge of the mode lifetimes which are not well known for an evolved K giant star like 42 Dra. Assuming a mode lifetime comparable to the sun (≈ 2.9 days) results in a velocity amplitude of ≈ 15 m s $^{-1}$. However, red giant stars can have mode lifetimes of up to a month (De Ridder et al. 2009) or even more for a giant like 42 Dra. This results in a predicted oscillation amplitude of ≈ 50 m s $^{-1}$. Thus the observed amplitudes for the short term variations in 42 Dra are entirely consistent with stellar oscillations.

5. Discussion

Precise RV measurements of 42 Dra taken between 2004 and 2008 reveal variations with a period of 479 d and an amplitude of 110 m s $^{-1}$ that were attributed to a planetary companion (D09). This detection passed all the standard tests for planet confirmation. There were no H α variations indicative of activity. HIPPARCOS photometry and line bisectors showed variations with a period of 690-d that were well separated from the orbital period of the purported planet. Furthermore, the 479-d variations were coherent and present for at least four years. As a planet detection, 42 Dra b was as solid as many other claimed planets. The original conclusion by D09 seemed reasonable.

Additional RV monitoring of this star tells another story. RV measurements taken between 2008 and 2011 show that the K -amplitude decreased abruptly from about 100 m s $^{-1}$ to 27 m s $^{-1}$. Furthermore, if one only considers the RV data from

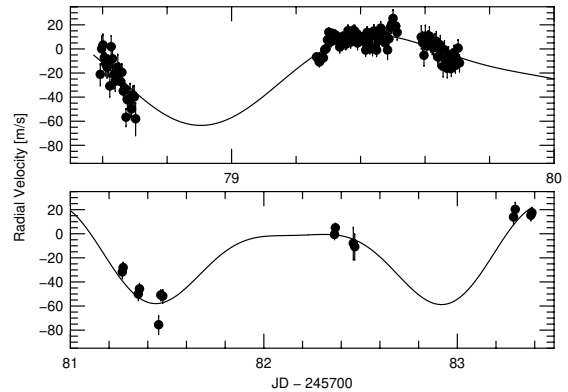


Fig. 8. Short term RV variability of 42 Dra over several nights. The curve is a two-period fit with period, $P_1 = 1.3$ d, amplitude $K_1 = 79.3$ m s $^{-1}$; $P = 0.82$ d, $K_2 = 49.2$ m s $^{-1}$.

2008 to 2011, a peak in the periodogram appears at the wrong period. Simulations using the published orbital solution sampled in the same manner as the real data indicate that we should have found the planet signal in the subset data. Even in the 2008 – 2011 data there were indications that the planet was not real which was finally confirmed by the DIRBE photometry that showed significant periodic variations exactly at the orbital period of the planet

A frequency analysis of the full data set spanning 2004 – 2018 reveal a possible origin of the amplitude variations. This results in an additional period at 530 d. The beating of these two closely spaced periods can mimic amplitude variations (Fig. 4). It is impossible for these two periods to be planetary companions as this would require giant planets in nearly the same orbit. This system would be dynamically unstable.

It is beyond the scope of this paper to perform a detailed dynamical analysis. However, the stability can be estimated by the Hill radius, r_H , given by:

$$r_H \approx a \left(\frac{m}{3M} \right)^{1/3}$$

where a and m are the semi-major axis and mass of the smaller body, and M the mass of the star. A minimum separation of approximately $3.5 R_H$ is widely accepted as the minimum requirement for long-term stability. Using the amplitudes and periods from Table 5, our two hypothetical planets would have masses of approximately $3.2 M_{Jup}$ and $2 M_{Jup}$ and semi-major axes of 1.24 AU and 1.32 AU, respectively. Each planet has a Hill radius $r_H \approx 0.1$, comparable to the minimum separation. This suggests an unstable system.

Gladman (1993) also established the stability of a three body system based on the Hill criterion. Consider a two-planet system with mass m_1 and m_2 in orbit around a star of mass M . We can denote the semi-major axis of the outer planet by $a = 1 + \Delta$, where Δ is the fractional separation. If the mass ratios of the two planets with respect to the host star are given by μ_1 and μ_2 then orbits are most likely stable if

$$\Delta > 2.4(\mu_1 + \mu_2)^{1/3}$$

For the hypothetical planets of 42 Dra, $\Delta = 0.08$, $\mu_1 = 2.8 \times 10^{-3}$ and $\mu_2 = 1.9 \times 10^{-3}$. In this case Δ is less than $2.4(\mu_1 + \mu_2)^{1/3} = 0.4$, so the system is unstable.

It is not clear what the nature of the 479-d RV period is, the one initially attributed to a companion. One candidate would be rotational modulation by surface features. So far at least five periods have been identified in 42 Dra: ≈ 480 d (RV and DIRBE photometry), 535 d (RV), 294 d (RV), 690 d (HIPPARCOS photometry and BVS) and 170 d (DIRBE photometry). These are not harmonics of each other which is typical for rotational modulation, so only one can be the rotation period. The fact that the 479-d period is also seen in the DIRBE photometry suggests that this may be due to rotational modulation by surface features. However, photometric variations were also seen at 690-d in the HIPPARCOS photometry, albeit with lower significance.

One can estimate the rotational period from the radius and the rotational velocity of the star. Jofre et al. (2015) measured a projected rotational velocity $v \sin i = 1.76 \pm 0.45 \text{ km s}^{-1}$ which yields a maximum rotation period of 554 ± 142 d. This is consistent with either the 479-d period or the 690-d period found in the HIPPARCOS photometry and the BVS. We cannot be certain which of these is the rotation period.

Given the large number of periods which may be present in the RV and photometry of 42 Dra, the simplest explanation is that these arise from stellar oscillations. Long period RV variations with comparable periods have been found in other evolved stars. For example, Jorissen et al. (2016) found RV variations with a K-amplitude of 540 m s^{-1} and a period $P = 285$ d in the Carbon-enhanced metal poor (CEMP) star HE 0017+0055. Since variability with similar periods were found in other CEMP stars, they proposed that the RV variations may be due to envelope oscillations. Oscillatory convective modes were suggested for the long-period RV variations in γ Dra (Hatzes et al. 2018). Only additional studies, both observational and theoretical are needed to confirm the type of oscillations seen in 42 Dra.

42 Dra is yet another case where all the standard tools of planet confirmation of an RV discovery seem to have failed. This only emphasizes that when confirming such long period RV variations in K giant stars one needs to look not only at as many ancillary measurements as possible (which may still fail), but also to take measurements spanning more than a decade to search for amplitude variations and closely spaced periods. Long-term monitoring of K giants with planet candidates may be essential for confirmation of the planet hypothesis. Additionally, one can use RV measurements taken at infrared wavelengths to confirm planet detections around K giant stars (Trifonov et al. 2015).

Long-period RV variations attributable to stellar oscillations have been found in several K giant stars. This raises the question: “*How many planets around evolved stars are false?*”. The “fake” planets around evolved IM stars may skew the statistics on the frequency of giant planet formation around more stars more massive than the sun which could have implications for planet formation theories.

It is worth noting that producing “real” planets also has implications in public outreach. Recently, the International Astronomical Union (IAU) has started to assign proper names

to exoplanets that have been discovered, many of these with the RV method. The planet around 42 Dra was assigned the name *Orbitar*¹ which now would have to be retracted. This is not the first planet to be refuted, nor the last. Besides K giant stars this has happened with the “disappearance” of planets around the main sequence stars GL 581 (Forveille et al. 2011; Robertson et al. 2014) and α Cen B (Hatzes 2013; Rajpaul et al. 2016). The $3.2 M_{\oplus}$ planet claimed around Barnard’s Star (Ribas et al. 2018) was later shown to be a false positive due to the one-year alias of an stellar activity signal (Lubin et al. 2021).

We welcome the effort to broaden the appeal of the exciting field of exoplanet research to the public and 42 Dra b (*Orbitar*) shows the public that science is not always perfect. Scientists sometimes get it wrong in pursuit of the truth. There will continue to be cases where forms of intrinsic variability (sometimes unknown) can mimic a planet signal. Astronomers and the public should realize that many RV planet discoveries are still candidates that must be confirmed by independent methods. We note that the Gaia mission can provide astrometric observations that could confirm the planetary nature of the long period RV variations in K giant stars. A naming convention is commendable, but it is more important that the IAU adopt a set of criteria that exoplanet discoveries have to pass before they are declared as bona fide planets. The complex RV variability of K giants only highlights our ignorance regarding stellar phenomena in these stars. Continued studies of these stars are required to sort out which variations are companions, and which are due to intrinsic stellar variability and these may require dedicated surveys lasting ten years or more.

Acknowledgements. This research has made use of the SIMBAD database operated at CDS, Strasbourg, France. APH acknowledges the support of DFG grants HA 3279/5-1 and HA 3279/8-1.

References

- Abdurro’uf, Accetta, K, Aerts, C. et al. 2022, ApJS, 259, 35
 Baines, E.K., Armstrong, J.T., Schmitt, H.R. et al. 2018, AJ, 155, 30
 De Ridder, J., Barban, C, Baudin, F. et al. 2009, Nature, 459, 398
 Döllinger, M.P., Hatzes, A.P., Pasquini, L. et al. 2007, A&A, 472, 649
 Döllinger, M.P., Hatzes, A.P., Pasquini, L. et al. 2009a, A&A, 499, 935
 Döllinger, M.P., Hatzes, A.P., Pasquini, L. et al. 2009b, A&A, 505, 1311 (D09)
 Forveille, T., Bonfils, X., Delfosse, X. et al. 2011, eprint arXiv:1109.2505
 Frink, S., Mitchell, D.S., Quirrenbach, A. et al. 2002, ApJ, 576, 478
 Gaia collaboration, Brown, A.G.A., Vallenari, A. et al. 2021, A&A, 649, 1
 Gladman, B. 1993, Icarus, 106, 247
 Gontcharov, G.A., Mosenkov, A.V. 2018, MNRAS, 475, 1121
 Hatzes, A. P. 2013, ApJ, 770, 133

¹ nameexoworlds.iau.org

- Hatzes, A. P. 2019, *The Doppler Method for the Detection of Exoplanets*, by Hatzes, A.P. ISBN: 978-0-7503-1687-3. IOP ebooks. Bristol, UK: IOP Publishing
- Hatzes, A. P. & Cochran, W. D. 1993, *ApJ*, 413, 339
- Hatzes, A. P., Cochran, W. D. & Bakker, E.J. 1998, *ApJ*, 408, 380
- Hatzes, A. P., Guenther, E. W., Endl, M. et al. 2005, *A&A* 437, 743
- Hatzes, A. P., Cochran, W. D., Endl, M. et al. 2015, *A&A*, 580, 31
- Hatzes, A. P., Cochran, W. D., Endl, M. et al. 2018, *A&A*, 155, 120
- Høg, E., Fabricius, C., Makarov, V.V. et al. 2000, *A&A*, 355, 27
- Huélamo, N. Figueira, P., Bonfils, X, et al. 2008, *A&A*, 489, 9
- Jofre, E., Petrucci, R., Saffe, C. et al. 2015, *A&A*, 574, 50
- Johnson, J.A., Fischer, D.A., Marcy, G.W. et al. 2007, *ApJ*, 665, 785
- Jones, M. I., Jenkins, J.S., Rojo, P., Melo, C.H.F. 2011, *A&A*, 536, 71
- Jorissen, A., Van Eck, S., Van Winckel, H. et al. 2016, *A&A*, 586, 158
- Kjeldsen, H. & Bedding, T.R. 1995, *A&A*, 87, 106
- Kjeldsen, H. & Bedding, T.R. 2011, *A&A*, 529, 8
- Khalatyan, A., Anders, F., Chiappini, C. et al. 2024, *A&A*, 691, 98
- Kuschnig, R., Weiss, W.W. Gruber, R. et al. 1997, *A&A*, 328, 544
- Lambert, D. L. 1987, *ApJS*, 65, 255
- Lee, B.-C., Mkrtichian, D. E., Han, I., Park, M.-G., Kim, K.-M. 2012, *A&A*, 548, 118
- Lubin, J., Robertson, P., Stefansson, G. et al. 2021, *AJ*, 162, 61
- Murdoch, K. A., Hearnshaw, J.B. & Clark, & M. 1993, *ApJ*, 413, 349
- Niedzielski, A., Goździewski, Wolszczan, A. et al. 2009 *ApJ*, 693 276
- Paegert, M., Stassun, K.G., Collins, K.A. et al. 2021, eprint arXiv:2108.04778
- Price, S.D., Smith, B.J., Kuchar, T.A. et al. 2010, *ApJ Supp.*, 190, 203
- Queloz, D., Henry, G. W., Sivan, J. P. et al. 2001, *A&A*, 379, 279
- Rajpaul, V., Aigrain, S., Roberts, S. 2016, *MNRAS*, 456, 6
- Reichert, K., Reffert, S., Stock, S. et al. 2019, *A&A*, 625, 22
- Ribas, I., Tuomi, M., Reiners, A. et al. 2018, *Nature*, 563, 365
- Robertson, P., Mahadevan, S., Endl, M., Roy, A. 2014, *Science*, 345, 440
- Sato, B., Izumiura, H., Toyota, E. et al. 2008, *PASJ*, 60, 539
- Scargle, J. D. 1982, *ApJ*, 263, 835
- Setiawan J. Hatzes, A.P., von der Lühse, O. et a. 2003, *A&A*, 398, 19
- Setiawan J., Henning, Th., Launhardt, R. et al. 2008 *Nature*, 451, 385
- Stock, S., Reffert, S., Quirrenbach, A. 2018, *A&A*, 616, 33
- Trifonov, T., Reffert, S., Zechmeister, et al. 2015, *A&A*, 582, 54
- Wittenmyer, R.A., Endl, M., Wang, L. et al. 2001, *ApJ*, 743, 184
- Yu, J., Khanna, S., Themessl, N., et al. 2023, *ApJS*, 264, 41
- Zechmeister, M., Köhler, J. & Chamarthi, S. 2021, record ascl:2108.006

Parameter	Value	Julian Day	RV (m s ⁻¹)	σ (m s ⁻¹)
mag_B^1	6.005 ± 0.014 mag	2453128.4179	-63.53	4.39
mag_V^2	4.823 ± 0.009 mag	2453192.5234	-128.00	4.87
parallax ³	11.056 ± 0.0841 mas	2453193.4023	-136.67	3.99
[Fe/H] ⁴	-0.4326 ± 0.01 dex	2453238.4101	-71.90	3.22
E(B-V) ⁵	0.05 ± 0.01 mag	2453301.3281	37.73	4.10
A_V^6	0.17 ± 0.01 mag	2453302.5234	58.13	6.00
M	$1.07 \pm 0.01 M_\odot$	2453303.4179	32.20	4.25
R	$19.17^{+0.3}_{-0.17} R_\odot$	2453304.2578	54.08	3.74
$\log g$	1.9 ± 0.02 cm/s ²	2453419.7109	66.50	3.70
$\log(\tau$ [yr])	9.81 ± 0.04	2453460.6171	87.46	4.78
L	$129.26^{+1.77}_{-1.05} L_\odot$	2453461.6367	85.11	4.02
T	$4449.08^{+11.40}_{-16.72}$ K	2453476.5234	35.30	3.49

Table 1. Stellar parameters for 42 Dra. The input values for SPOG+ (above the line) are taken from: (1, 2) Høg et al. (2000), (3) Gaia collaboration et al. (2021), (4) Abdurro’uf et al (2022), (5, 6) Gontcharov & Mosenkov (2017). Those parameters derived with SPOG+ are listed below the line.

List of Objects

‘42 Dra’ on page 1

2453481.5664	54.53	5.09
2453482.5742	71.82	5.13
2453483.5078	78.34	4.31
2453484.5273	16.88	5.19
2453637.3281	-100.05	3.61
2453654.4453	-54.45	3.83
2453655.5195	-63.21	2.82
2453656.5390	-82.01	2.78
2453657.5234	-86.01	3.05
2453899.5312	59.13	6.01
2453900.4804	88.22	5.40
2453901.5703	87.32	5.05
2453904.5039	112.20	5.43
2453873.0468	102.46	3.37
2453995.3398	72.88	3.78
2454041.2890	-17.56	3.41
2454047.2656	-3.62	6.70
2454097.2226	-82.45	4.04
2454136.6992	-152.06	4.05
2454118.6835	-96.67	2.49
2454182.1562	-166.03	2.92
2454309.3828	38.85	4.06
2454313.3750	76.34	4.69
2454330.3281	89.84	4.36
2454337.3359	75.80	3.73
2454660.4882	-9.22	1.86
2454663.5000	-46.89	1.80
2454692.5156	-50.31	2.19
2454694.5312	12.14	2.22
2454695.4218	-50.92	2.37
2454637.7500	-50.68	3.84
2454529.6445	-21.38	12.39
2454530.5234	-95.68	13.20
2454601.4921	-86.51	2.60
2454611.5273	-36.67	3.58
2454727.5312	-33.96	3.78
2454728.4335	-18.75	3.42
2454732.3359	-29.71	10.96
2454778.6562	-37.18	3.00
2454779.4492	-8.61	3.60
2454781.3789	-60.49	2.93

Table 2. RV measurements for 42 Dra 2004 - 2011

Julian Day	RV (m s ⁻¹)	σ (m s ⁻¹)
2454782.4140	-16.40	3.92
2454783.3398	3.92	2.51
2454845.6640	-1.20	4.05
2454872.3359	35.04	13.11
2454875.5664	5.80	2.19
2454877.5898	12.25	1.53
2454952.5898	-17.91	6.70
2454953.5859	-5.82	3.41
2454954.5820	-13.88	3.78
2454959.3281	-7.92	5.74
2454960.5703	-9.52	3.97
2455000.4726	-33.91	6.84
2455001.4882	-38.54	3.40
2455002.4257	-81.78	3.20
2455003.5351	-66.32	2.97
2455004.4140	-49.38	3.33
2455034.5390	-28.14	6.40
2455035.3789	-45.51	3.99
2455037.4257	-66.52	4.17
2455038.4843	-70.20	2.61
2455039.5468	-35.91	2.82
2455050.3437	-46.22	3.33
2455051.3554	-57.22	4.37
2455057.3437	-40.42	2.52
2455150.6015	12.63	2.81
2455153.5625	-0.59	3.63
2455155.4687	-47.92	2.74
2455156.3437	-9.39	9.03
2455157.2968	5.85	3.57
2455158.4179	4.11	1.89
2455161.2656	-4.12	4.27
2455162.2851	-7.01	3.53
2455163.2890	37.15	4.27
2455168.2968	34.32	2.66
2455170.3203	-11.73	3.98
2455171.2226	33.40	3.63
2455173.2890	-20.36	2.86
2455175.3046	-12.73	2.43
2455192.1835	-1.52	3.10
2455193.2460	-4.85	4.85
2455194.3242	11.27	2.63
2455278.5546	15.51	4.72
2455352.3710	22.08	4.74
2455403.4765	11.57	3.84
2455450.5898	47.74	3.84
2455461.6171	31.69	3.93
2455463.4257	1.56	7.160
2455478.2578	-7.91	4.03
2455495.2421	32.37	3.77
2455496.3789	-8.00	3.84
2455549.5898	-53.38	10.20

Table 2. RV measurements for 42 Dra 2004 - 2011 (cont.)

Julian Day	RV (m s ⁻¹)	σ (m s ⁻¹)
2456875.4094	21.91	2.28
2456877.5337	-8.38	5.04
2456881.5527	-20.85	3.54
2456903.4301	-75.42	2.37
2456916.2838	-55.13	4.52
2457186.4182	100.69	4.72
2457187.4240	90.43	4.60
2457188.4137	126.42	4.08
2457189.4683	119.40	5.00
2457328.3674	14.82	6.07
2457329.2581	67.88	7.10
2457446.7115	-95.02	4.21
2457611.5435	-26.78	4.31
2457614.3892	6.14	2.92
2457619.4522	33.46	5.32
2457706.4234	108.65	5.21
2458156.7328	23.72	4.25

Table 3. RV measurements for 42 Dra 2014 - 2018

Parameter	Value
Period [days]	473.9 ± 4.0
T ₀ [JD-2450000]	2711.60 ± 32.7
K [m s ⁻¹]	65.8 ± 5.9
<i>e</i>	0.25 ± 0.007
ω [deg]	181.2 ± 19.8
<i>f</i> (<i>m</i>) [solar masses]	(1.27 ± 0.34) × 10 ⁻⁸
<i>m</i> sin <i>i</i> [<i>M</i> _{Jupiter}]	2.45 ± 0.21
<i>a</i> [AU]	1.18 ± 0.06

Table 4. Orbital solution of the purported planet around 42 Dra using the full RV data.

Period (d)	Amplitude (m s ⁻¹)	Phase	SNR	FAP
487.8 ± 0.9	79.3 ± 3.5	0.75 ± 0.01	6.9	5.3 × 10 ⁻¹⁸
534.8 ± 2.2	49.2 ± 3.5	0.39 ± 0.01	5.3	1.0 × 10 ⁻⁸
294.1 ± 0.2	20.7 ± 3.5	0.40 ± 0.03	4.7	3.7 × 10 ⁻⁶

Table 5. Frequencies found in the full RV data set.

Julian Day	RV (m s ⁻¹)	σ (m s ⁻¹)
2454778.5926	-21.08	8.86
2454778.5968	0.17	10.87
2454778.6011	3.30	9.11
2454778.6053	-7.21	9.36
2454778.6095	-12.59	9.41
2454778.6138	-15.28	8.48
2454778.6180	-13.76	8.72
2454778.6222	-30.75	8.80
2454778.6265	1.91	9.21
2454778.6307	-8.17	9.17

Table 6. Short-term RV measurements for 42 Dra (full table in electronic form)